Letters

A Family of Multi-Mode Rectifiers

Qunfang Wu, *Member, IEEE*, Wenjie Zhao, Qin Wang, *Member, IEEE*, and Lan Xiao, *Member, IEEE*

***Abstract*—Existing applications, such as photovoltaic systems and on-board power supplies, propose higher requirements for the gain range, efficiency, and power density of isolated dc/dc converters. However, the gain range of traditional isolated dc/dc converters is limited and the efficiency diminishes significantly when the input voltage mismatches. This article proposes a novel method to derive a family of multi-mode rectifiers based on basic structures, which is appropriate for many traditional isolated dc/dc converters. Each one can operate in various modes by adjusting the states of secondary switches. Combining the proposed rectifiers with different types of isolated converters, the input voltage range is widely expanded compared with conventional ones. Taking the *LLC* resonant converter with one of the proposed rectifiers as an example, a 250 W 38∼120 V input, 500 V output prototype is developed and tested, with a peak efficiency of 98.196%. Zero voltage switching and zero current switching are realized to ensure high efficiency. Compared with similar *LLC* converters with secondary rectifiers, the proposed one's own a much wider gain range and higher efficiency with fewer devices. Experimental results correspond to theoretical analysis and verify the effectiveness of the proposed rectifiers.**

***Index Terms*—Isolated dc–dc converter, *LLC* resonant converter, multi-mode switchable rectifier, wide input voltage range, zero voltage switching (ZVS).**

I. Introduction

With the promotion of applications and the improvement of design specifications, the requirements in the gain range and efficiency of isolated dc–dc converters have greatly increased. For example, in renewable power systems such as photovoltaic (PV) grid-connected systems, the output dc voltage of PV panels is converted to the dc bus or dc microgrid by using an isolated dc/dc converter. However, the output voltage of PV panels varies significantly when the lighting intensity and the number of battery panels are different. Moreover, the voltage of dc bus is usually high so that the turns ratio of the transformer needs to be increased to fulfil the demand of the high output voltage, which will increase the nonideality of the transformer, the voltage requirements of secondary devices, the total volume, etc. A commercial inverter product, for example, has a PV panel output voltage range lower than 120 V, and a dc bus voltage of 500 V, with a wide gain range. Thus, it is necessary to extend the gain range, enhance full-range efficiency, reduce power density, improve reliability and stability.

The modulation methods for traditional isolated dc–dc converters include pulsewidth modulation (PWM), phase-shift modulation (PSM), and pulse frequency modulation (PFM). For traditional converters adopting a single modulation method, the voltage gain range is limited and the efficiency diminishes significantly when the input voltage mismatches, especially for resonant converters. For example, the traditional *LLC* resonant converter must operate around the resonant frequency and the efficiency will be degraded if the switching frequency operates far away from the resonant frequency.

Thus, in recent years, there have been many techniques in expanding the gain range of traditional isolated dc–dc converters, including hybrid control strategies, accurate analysis and design methods, topological modifications, etc. Focusing on the various converters with topological modifications, they can be divided into three different subgroups, that is, primary inverter, transformer, and secondary rectifier. Among them, the most generalized and intuitive modifications are the secondary rectifier structures. In [11], a simple voltage doubler rectifier is used in the interleaved isolated Boost converter to realize a high voltage gain. In [12] and [13], the secondary rectifier structure is the controllable voltage doubler rectifier, which helps extend the gain range and realize the ZCS of secondary diodes.

However, the PWM and PSM converters are unable or difficult to achieve soft switching of all power devices, which limits the efficiency improvement, while the resonant converter become a popular choice in various applications for its high efficiency, high power density, and simple structure. Thus, there have been many studies on the secondary rectifiers of resonant converters especially the *LLC* converter, which has been widely used in various applications and the typical application scenarios include power supplies for servers, front-end converters for renewable power systems, battery chargers for electrical vehicles, etc. [1], [2]. Focusing on the studies of the *LLC* converter with rectifiers,

Manuscript received 9 May 2024; revised 26 June 2024 and 10 July 2024; accepted 20 July 2024. Date of publication 29 July 2024; date of current version 4 September 2024. This work was supported in part by the National Natural Science Foundation of China under Grant 62371233, in part by the Natural Science Youth Foundation of Jiangsu Province under Grant BK20210305, in part by the Fundamental Research Funds for the Central Universities under Grant NJ2023012 and Grant NJ2023014, and in part by Aviation Science Foundation Project under Grant 2022Z024052003 and Grant 20230058052001. *(Corresponding authors: Wenjie Zhao; Qunfang Wu.)*

The authors are with the School of Nanjing University of Aeronautics and Astronautics, Nanjing 210016, China (e-mail: wuqunfang@nuaa.edu.cn; wenjie.zhao@nuaa.edu.cn; wangqin@nuaa.edu.cn; xiaolan@nuaa.edu.cn).

Color versions of one or more figures in this article are available at https://doi.org/10.1109/TPEL.2024.3434549.

Digital Object Identifier 10.1109/TPEL.2024.3434549

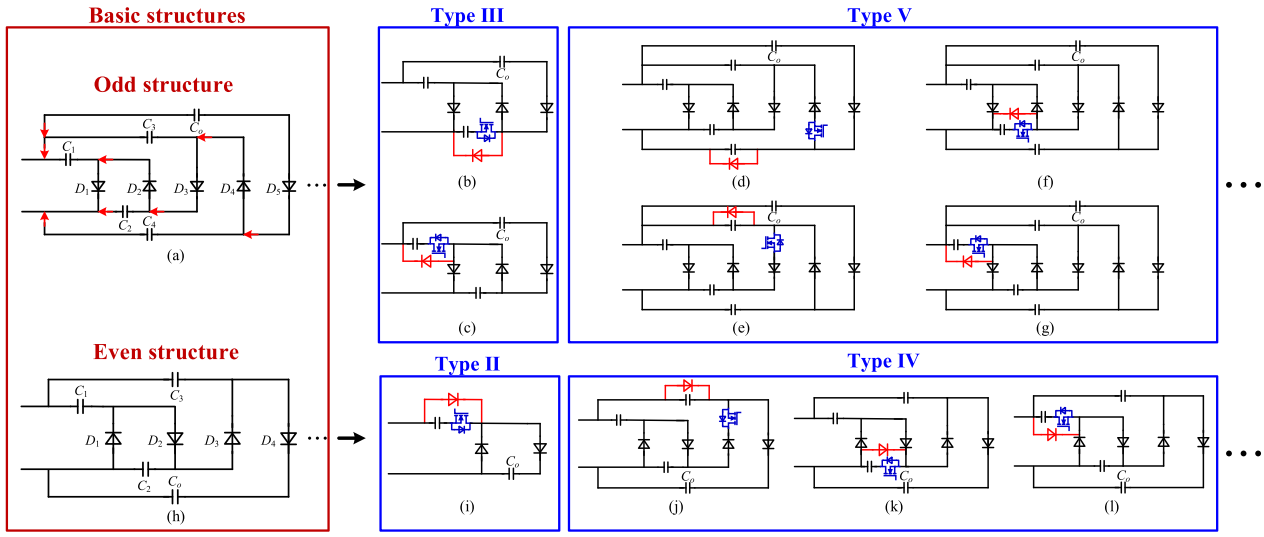

Fig. 1. Derivation processes and examples of single-switch multimode rectifiers.

in [5], [6], [7], and [8], various *LLC* converters with secondary multimode rectifiers have been proposed. For example, in [6], by changing the control strategy of the secondary switches, the rectifier can be set to operate in two modes with smooth mode switching, which extends the output voltage range. In [8], the conventional full-wave rectifier is replaced by a reconfigurable voltage multiplier rectifier operating in type-4, type-5, and type-6 modes, which can realize wide-range regulation of input voltage with guaranteed efficiency.

Although existing modifications for secondary rectifiers have some enhancements, the input voltage gain range and efficiency of the isolated dc–dc converters with existing rectifiers still cannot fully meet the demand in practice. To realize both the wide gain range and the all-around high efficiency, a family of multimode switchable rectifiers is proposed, which applies to many isolated PWM, PSM, and PFM dc–dc converters. The novelties and contributions of the article are as follows.

1) A novel derivation method of multi-mode rectifiers based on basic structures is proposed with a family of zero-switch, single-switch, and double-switch circuits.
2) Combining the *LLC* resonant converter with the multimode rectifiers, a family of converters with soft-switching of all power devices in different modes and a wide input voltage range is proposed for various applications.
3) The proposed a family of multimode rectifiers can be expanded to be combined with PWM, and PFM converters with a wider input voltage range than conventional ones, which provides references for the selection of primary converters and appropriate rectifiers in practical applications.

The rest of this article is organized as follows. Section II illustrates the derivation process of a family of multi-mode rectifiers. Section III compares the three types of converters with one of the rectifiers. Section IV provides a detailed analysis of the principles taking one of them as an example. Experimental results and comparisons are given in Section V. Finally, Section VI concludes this article.

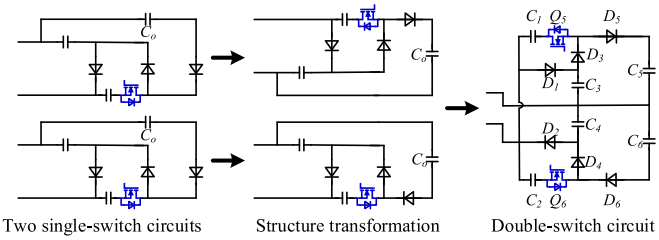

Fig. 2. Composition of the double-switch circuit.

II. Derivation Process of Rectifiers

A. Basic Structure

The proposed two types of basic structures can be seen in Fig. 1(a) and (h), which correspond to the odd and even structures respectively. The classification aims to ensure that the voltage of output capacitor C_o is positive at the top and negative at the bottom when C_o is moved to the far right as the output. The infrastructure of the two ones is consistent, as shown in Fig. 1(a). The incremental voltage multiplier is a combination of stages one by one, which means the new series combinations of one capacitor and one diode are continuously being connected to the previous capacitor and the input port, which makes the voltage of capacitors increase step by step.

In detail, when the input port of the structure is an ac sinusoidal voltage $V_{\text{in}}(t)$ with the peak value of V_{in}, the capacitors will be charged repeatedly through diodes in each positive and negative half cycle. Based on the two novel basic structures, basic circuits with an arbitrary voltage of C_o can be derived easily. For the example of the odd structure, the number of capacitors and diodes is odd. When the desired voltage of C_o is $3V_{\text{in}}$, three capacitors and diodes (C_1, D_1, C_2, D_2, C_o, D_3) will be needed to construct this circuit. After several switching cycles, C_1 will be charged to V_{in}, C_2 will be charged to $2V_{\text{in}}$, and C_o will be charged to $3V_{\text{in}}$. As a result, circuits with any odd voltage of C_o can be obtained from the odd basic structure easily. Similarly,

TABLE I
PART OF THE SINGLE-SWITCH CIRCUITS

Multiples	1/2	1/3	2/3	1/4	2/4	3/4	1/5	2/5	3/5	4/5
Diodes	3	3	4	5	4	5	6	6	5	6
Capacitors	2	3	3	4	4	4	5	5	5	5
Switches	1	1	1	1	1	1	1	1	1	1

basic circuits with any even voltage of C_o can be obtained based on the even structure, where the diodes are opposite to the odd one.

B. Zero-Switch and Single-Switch Circuits

Based on the basic structures, basic circuits with any single output voltage can be obtained. Combining two of these basic circuits derived from the basic structure, a family of zero-switch circuits with a single output voltage can be obtained. For example, the voltage-quadruple rectifier (VQR) can be composed of two basic circuits with an output voltage of $2V_{\rm in}$.

Furthermore, by adding an extra switch and diode to basic circuits, two-mode single-switch circuits can be developed, as shown in Fig. 1. For the circuit with the output voltage of $3V_{\rm in}$, which can operate in voltage-triple rectifier (VTR) mode, through adding extra components, it can be converted to two single-switch circuits, as shown in Fig. 1(b) and (c). In Fig. 1(b), this circuit can operate in voltage-doubler rectifier (VDR) and VTR modes, which means it can operate in multiples of 2 or 3. Besides, in Fig. 1(c), it can operate in voltage-single rectifier (VSiR) and VTR modes, which means it can operate in multiples of 1 or 3.

These two circuits constitute type III together, which means the maximum voltage they can generate is $3V_{\rm in}$. Similarly, other types of circuits can also be derived and part of the single-switch circuits are aggregated in Table I, where the first row represents the multiples of the output voltage that can be realized and others show the number of devices needed.

It is worth noting that the extra diode can be saved in converters with multiples of 1/3, 2/4, 3/5, etc. The diodes in intrinsic circuits can play the same role as the extra diode.

C. Double-Switch Circuit

Based on the two-mode single-switch circuits, two single-switch circuits can be combined to form a double-switch circuit. As shown in Fig. 2, two circuits with the function of 1 or 3 can be combined into a double-switch circuit. In this case, the upper part can operate in VSiR and VTR modes, while the lower part can also operate in VSiR and VTR modes by adjusting the state of the switch.

Here, 0 and 1 are introduced to indicate the state of each switch, where 1 means the switch is turned ON and 0 indicates the switch is turned OFF. As shown in Fig. 3, when the two switches are both turned ON, the two parts operate in VTR mode and thus the double-switch circuit operates in voltage-sixfolder rectifier (VSR) mode. When switches are 10 or 01, the circuit can both operate in VQR mode, which means only one of them needs to be selected.

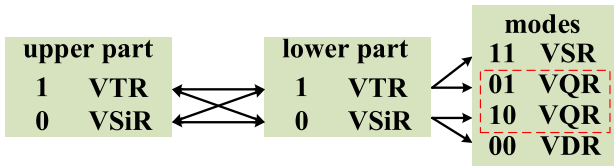

Fig. 3. Schematic diagram of working modes.

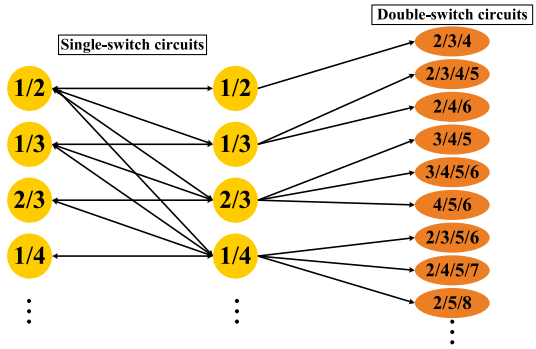

Fig. 4. Double-switch circuits composition logic diagram.

Furthermore, a series of double-switch switchable rectifiers can be obtained by combining two single-switch circuits previously derived, as shown in Fig. 4. In Table II, a comparison of device quantity and multiples among the proposed double-switch circuits is made. Among them, the circuit with the multiple of 4/5/6 has been proposed in [8] and the circuit in [7] with the multiple of 3/5/6 is similar to the structure with the multiple of 3/4/5/6.

The zero-switch and double-switch mutimode rectifiers can be connected to the secondary side of isolated dc–dc converters with normal operating. However, the single-switch circuits in Fig. 1(b)–(g) and (i)–(l) are not recommended to be directly connected to the secondary side. Because some of the single-switch circuits offer no path for current to return when the switch is off and some cause errors in circuit operation.

III. COMPARISON OF CONVERTERS WITH RECTIFIERS

A comprehensive comparison of the resonant converter, PWM converter, and PSM converter has been given in Table III. The typical converters of the three types of isolated dc–dc converters are the *LLC*, flyback and phase-shifted full bridge (PSFB) converter. Besides, the multimode rectifier is the one mentioned in Section II, which can operate in VDR, VQR, and VSR modes.

The converters with the new rectifier all own a wide input voltage range. The input range of flyback and PSFB with the rectifier is much wider than *LLC* because these two types of modulation methods can achieve wider voltage gain. Besides,

TABLE II
FAMILY OF DOUBLE-SWITCH CIRCUITS

Combination method	1/2+1/2	1/2+1/3	1/2+2/3	1/3+1/3	1/3+2/3	2/3+2/3	1/2+1/4	1/2+2/4	1/2+3/4	…
Diodes	6	6	7	6	7	8	8	7	8	…
Capacitors	4	5	5	6	6	6	6	6	6	…
Switches	2	2	2	2	2	2	2	2	2	…
Multiples	2/3/4	3/4/5	3/4/5	2/4/6	3/4/5/6	4/5/6	2/3/5/6	3/4/5/6	4/5/6	…

TABLE III
COMPARISON OF THREE TYPES OF ISOLATED DC–DC CONVERTERS WITH THE RECTIFIER

	LLC	Flyback	PSFB
Modulation	PFM	PWM	PSM
Modes	2/4/6	2/4/6	2/4/6
Turns ratio	0.25	0.5	0.1
Input voltage (V)	38~120	20~150	38~170
Output voltage (V)	500	500	500
Output power (W)	250	250	250
Current stresses of diodes (A)	0.5	0.5	0.5
Max voltage stresses of diodes(V)	500	500	500
Max voltage stresses of capacitors(V)	1000	500	500
Max voltage stresses of switches(V)	1000	500	500
Primary switches	ZVS ON	Hard switching	ZVS ON
Secondary switches	Hard switching	Hard switching	Hard switching
Secondary diodes	ZCS OFF	Hard switching	Hard switching

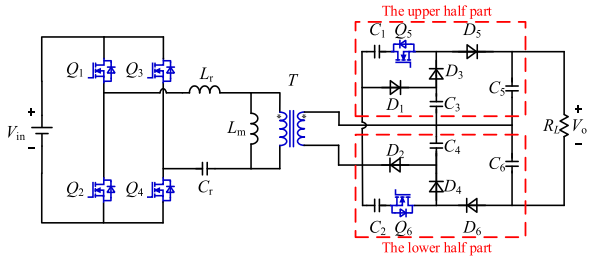

Fig. 5. Topology of the proposed *LLC* converter with one of the double-switch circuits.

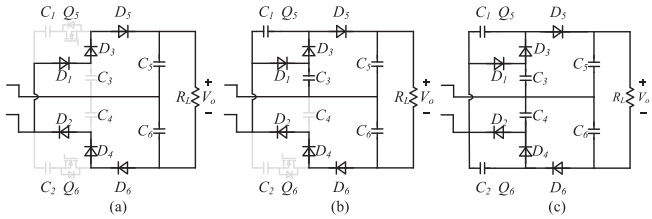

Fig. 6. Equivalent circuit modes. (a) VDR mode. (b) VQR mode. (c) VSR mode.

the max voltage stresses of the components in flyback and PSFB are the same with or smaller than those in the *LLC* due to the differential transformer output voltage.

However, the power devices of flyback are all hard switching, which will cause significant losses. Besides, only the primary switches in PSFB realize soft switching, which means losses of secondary diodes will be large if more diodes are used. So, for Flyback and PSFB, new rectifiers with few diodes are proper choices, including some of the zero-switch, single-switch, and double-switch rectifiers. For the *LLC* converter, the soft switching of primary switches and secondary diodes are both realized. So, it is easy to ensure the peak and all-range efficiency.

IV. ANALYSIS OF PROPOSED CONVERTERS

Combining the multimode rectifier mentioned in Section II with the *LLC* resonant converter and choosing a full-bridge structure as an example to explain the operating principle in detail.

A. Topology Description

The circuit configuration of the proposed *LLC* converter can be seen in Fig. 5, where the secondary side is changed from the conventional full-wave rectifier to the new structure. The Q_1, Q_2, Q_3, and Q_4 constitute the primary full-bridge structure and the resonant tank consists of the L_r, L_m, C_r, which are the same as the *LLC* converter. The new rectifier is composed of two symmetrical upper and lower parts with two MOSFETs, six diodes, and six capacitors. It is connected to the primary side through a transformer with a simpler composition and fewer turn ratios. Besides, the turns ratio of the transformer is 1:k.

B. Voltage Gain

The secondary rectifier consists of two single-switch circuits that can be set to work in three modes: VDR mode; VQR mode; and VSR mode. According to the input voltage, the converter can switch among three modes by adjusting the states of the switches. When the switching frequency f_s is equal to the resonant frequency f_r, the detailed description of the three modes can be seen as follows.

1) *VDR Mode:* As shown in Fig. 6(a), Q_5 and Q_6 are both turned OFF so that C_1 and C_2 are not involved in the operation. Besides, C_5 is charged to $kV_{\rm in}$ through D_1, D_3, D_5 and C_6 is charged to $kV_{\rm in}$ through D_2, D_4, D_6. In this mode, the output voltage V_o is $2kV_{\rm in}$ which is two times the output voltage of the full-bridge *LLC* converter with center-tapped full-wave rectifier.
2) *VQR Mode:* As shown in Fig. 6(b), Q_5 is turned on and Q_6 is also turned OFF so that C_1 participates in the operation. Besides, C_6 is still charged to $kV_{\rm in}$ through D_2, D_4, D_6. Significantly, in the upper half part, C_3 is firstly charged to $kV_{\rm in}$ through D_1, and then C_1 is charged to $2V_{\rm set}$ through

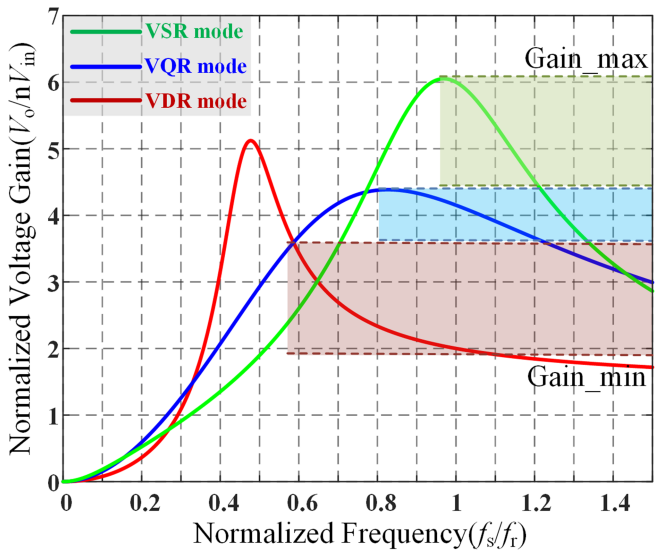

Fig. 7. Voltage gains versus normalized frequency.

D_3, C_3. Finally, C_5 is charged to $3kV_{\text{in}}$ through D_1, D_3, and D_5 and thus the output voltage V_o in this mode is $4kV_{\text{in}}$ which is two times the output voltage of the circuit in VDR mode.

3) *VSR Mode:* As shown in Fig. 6(c), Q_5 and Q_6 are both turned on so that C_1 and C_2 participate in the operation. The operating principles and output voltages of the upper and lower half part are the same as the upper half part in VQR mode. Thus, C_5 and C_6 are both charged to $3kV_{\text{in}}$ and the output voltage V_o in this mode is $6kV_{\text{in}}$ which is three times the output voltage of the circuit in VDR mode.

Thus, the voltage gains of the proposed *LLC* converter when f_s is equal to f_r can be seen as follows:

$$V_o = \begin{cases} 2kV_{\text{in}} & \text{VDR mode} \\ 4kV_{\text{in}} & \text{VQR mode} \\ 6kV_{\text{in}} & \text{VSR mode} \end{cases}. \tag{1}$$

Besides, the curve of the voltage gain versus the f_n by using the first harmonic approximation method is shown in Fig. 7. The voltage gain of the proposed converter and the equivalent input resistance of the resonant tank is

$$\mathrm{M}(f_{\mathrm{n}}) = \frac{m}{\sqrt{\left[\left(1-\frac{1}{f_{\mathrm{n}}{}^2}\right)Q_e f_{\mathrm{n}}\right]^2 + \left[\left(1-\frac{1}{f_{\mathrm{n}}{}^2}\right)\frac{1}{L_{\mathrm{n}}}+1\right]^2}} \tag{2}$$

$$\mathrm{Z} = jw_nL_r + \frac{1}{jw_nC_r} + \frac{jw_nR_{ac}L_m}{R_{ac}+jw_nL_m} \tag{3}$$

where

$$m=2 \quad Q_e = 2^2\frac{Z_o}{R_{ac}} \quad \text{VDR mode}$$

$$m=4 \quad Q_e = 4^2\frac{Z_o}{R_{ac}} \quad \text{VQR mode}$$

$$m=6 \quad Q_e = 6^2\frac{Z_o}{R_{ac}} \quad \text{VSR mode}$$

TABLE IV
COMPARISON OF CURRENT AND VOLTAGE STRESSES

	Shang et al. [8]	Alaql et al. [7]	Proposed
Modes	4/5/6	3/5/6	2/4/6
Output voltage	V_{o}	V_{o}	V_{o}
Output power	P_{o}	P_{o}	P_{o}
Current stresses of diodes	I_{o}	I_{o}	I_{o}
Max voltage stresses of diodes	$2V_{\text{o}}/3$	$2V_{\text{o}}/3$	$V_{\text{o}}/2$, V_{o}
Max voltage stresses of capacitors	$V_{\text{o}}/2$	$2V_{\text{o}}/3$	$V_{\text{o}}/2$, $2V_{\text{o}}$
Max voltage stresses of switches	$V_{\text{o}}/2$	$2V_{\text{o}}/3$	$2V_{\text{o}}$

$$L_n = \frac{L_m}{L_r}, f_n = \frac{f_m}{f_r}, Z_o = \sqrt{\frac{L_r}{C_r}}, R_{ac} = \frac{8k^2{U_o}^2}{\pi^2 P_o}. \tag{4}$$

C. Voltage and Current Stresses

The stresses of the different rectifiers with *LLC* converter are necessary to be calculated and simulated. The detailed comparison between the proposed one and other rectifiers with the same resonant tank, V_o and P_o is given in Table IV.

The voltage and current stresses are difficult to be accurately calculated in steady-state, so the stresses are roughly determined through simulation. The current stresses of diodes in all the rectifiers are I_o when V_o and P_o are the same. The max voltage stresses of diodes, switches, and capacitors of the proposed one are V_{o}, $2V_o$, and $2V_o$ which are larger than the others. However, only C_1, and C_2 withstand a high voltage as $2V_o$ in VDR mode while the voltage stresses of other capacitors are $V_o/2$, which is the same as or smaller than others. Besides, in VDR mode, only the voltage stresses of D_1, and D_2 are V_o while the others' are $V_o/2$. The current stresses of switches are difficult to describe quantitatively while the current is within $2I_o$ in simulation.

The voltage and current stresses of components in the rectifiers are related to the operating mode, circuit structure, etc. Adopting the proposed derivation method, a family of multi-mode rectifiers can be obtained. Thus, many rectifiers of them may exhibit lower stress characteristics, which decreases the costs and improves stability.

V. EXPERIMENTAL RESULTS AND COMPARISON

Finally, a 250 W prototype of the proposed *LLC* converter adopting PFM was implemented for experimental verification. The circuit parameters are listed as follows: V_{in}: 38–120 V; $V_{\text{o}} =$ 500 V; $P_{\text{o}} = 250$ W; $f_r = 100$ kHz; $f_{\text{s}} =$ 60–120 kHz; k: 46:100; $L_r = 16$ μH; $C_r = 159$ nF; $L_m = 60$ μH; C_1–$C_6 = 1$ μF. The steady-state waveforms of the converter in three modes can be seen in Fig. 9(a), (b), and (c), respectively, and the architecture of the experimental circuit can be seen in Fig. 8. In these modes, the ZVS ON of primary switches and the ZVS OFF of the secondary diodes are both realized. Fig. 9(d) shows the transition waveform from VQR to VDR mode. It can be seen that the smooth mode transition is achieved.

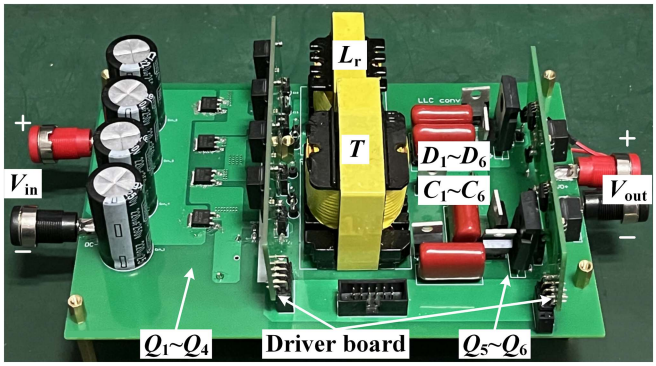

Fig. 8. Photograph of the implemented prototype.

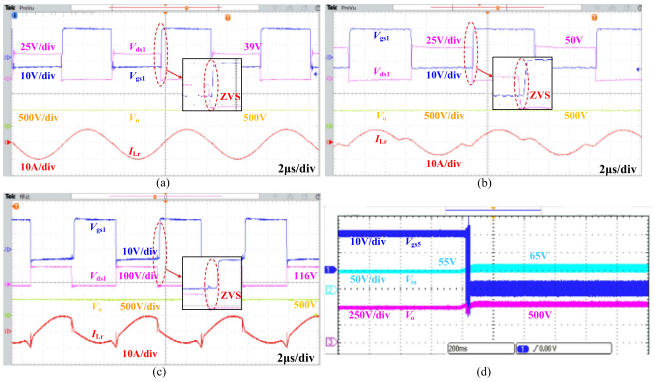

Fig. 9. Experimental waveforms. (a) $V_{in} = 39$ V in VSR mode. (b) $V_{in} = 50$ V in VQR mode. (c) $V_{in} = 116$ V in VDR mode. (d) Experimental voltage waveform of mode transition from VQR mode to VDR mode.

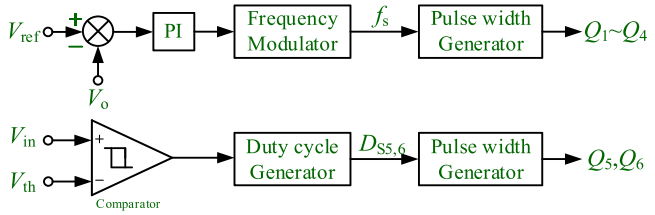

Fig. 10. Control block diagram of the proposed converter.

The control block diagram of the proposed converter is shown in Fig. 10. The output voltage is regulated with closed-loop control by varying the switching frequency of the Q_1~ Q_4 switches in each mode, while the operation mode and structure of the proposed converter are determined by the duty cycle of the switches Q_5 and Q_6. Determine the required operating mode of the proposed circuit by comparing the input voltage with the threshold voltage, so the duty cycle of Q_5 and Q_6 is obtained.

Fig. 11 shows the input voltage range in three modes and the threshold voltage should be set to 49 and 68 V according to the efficiency. When the input voltage is lower than 49 V, the converter will operate in VSR mode. Besides, when the input voltage is lower than 68 V and larger than 49 V, the converter will operate in VQR mode, meanwhile, the mode transformation accompanies the turning ON of Q_5. When the

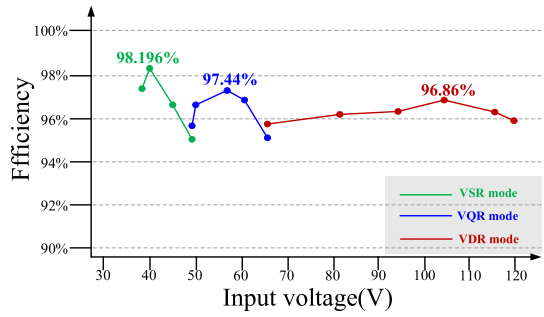

Fig. 11. Measured efficiency versus input voltages.

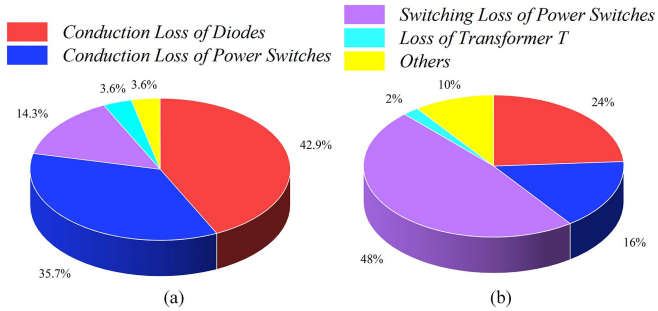

Fig. 12. Loss distribution under the operating conditions with (a) $V_{in} = 38$ V, $V_o = 500$ V in VQR mode, total loss: 5 W. (b) $V_{in} = 120$ V, $V_o = 500$ V in VDR mode, total loss: 10 W.

input voltage is larger than 68 V, the converter will switch to VDR mode. From the curves of the measured efficiency versus input voltage, the proposed converter operates efficiently in a wide input voltage range, with a peak efficiency of 98.196% and valley efficiency of 95.18%. The peak efficiency is higher than any other existing converters and the valley efficiency is still up to 95.18% which is higher than those in [7] and [8]. Fig. 12 shows the loss distribution of the experimental prototype. The losses of diodes and switches account for the most significant parts, which are 92.9% and 88% in Fig. 12(a) and (b), respectively. The conduction losses of the six secondary diodes are more than 20% and even up to 42.9% of the total loss. However, the output current is quite small so the efficiency of the entire prototype in these operating modes is higher than 96% which still performs well. Besides, when V_{in} increases, the switching losses of power switches will increase, which causes a decrease in efficiency. So, when V_{in} is 120 V, the switching losses of power switches account for 48% of the total loss, which is much higher than those in Fig. 12(a). The calculated results are consistent with the measured results.

Besides, the required number of devices is relatively large when the rectifier can be set to work in many modes. Therefore, if the gain range required in some industrial scenarios is not so wide, a simpler voltage multiplier is more appropriate, such as VDR and VQR, which are also included in the derivation method.

Fig. 13 shows the curves of the measured efficiency versus output power under different input voltages. As the output power decreases, the efficiency of the converter also decreases in three

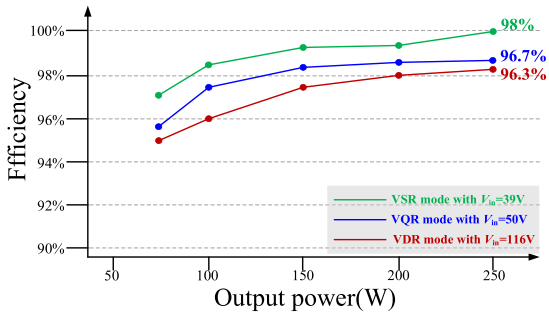

Fig. 13. Measured efficiency versus output power with $V_{\rm in} = 39$ V in VSR mode, $V_{\rm in} = 50$ V in VQR mode, $V_{\rm in} = 116$ V in VDR mode.

TABLE V
COMPARISON WITH EXISTING MULTIMODE CONVERTERS

	Shang et al. [8]	Alaql et al. [7]	Alaql et al. [5]	Proposed
Modulation	PFM	PFM	PFM	PFM
Secondary diodes	8	8	7	**6**
Secondary capacitors	6	6	5	**6**
Secondary switches	2	2	2	**2**
Modes	4/5/6	3/5/6	3/4/5	**2/4/6**
Turns ratio	0.25	0.48	0.53	0.46
Input voltage (V)	25~51	30~80	35~90	**38~120**
Output voltage (V)	760	500	500	500
Resonant frequency (kHz)	100	100	100	100
Output power (W)	300	250	250	250
Frequency range (kHz)	75-100	70-110	67-100	60-120
Peak efficiency (%)	96.1	96	98	**98.196**
Valley efficiency (%)	94.3	94.5	95.5	**95.12**

modes. However, the valley efficiency is still up to 95% when $V_{\rm in} = 116$ V and $P_{\rm o} = 75$ W.

A comprehensive comparison between the proposed topology and other similar topologies with multimode rectifiers under PFM is made, as given in Table V. As indicated, the proposed converter exhibits a much wider input voltage range with fewer secondary diodes and capacitors, which is a better alternative for wide input applications including PV systems.

VI. CONCLUSION

In this article, a novel method to derive a family of *LLC* converters with multimode switchable rectifiers based on basic structures is proposed, which is appropriate for many isolated dc–dc converters. Each rectifier can operate in various modes by adjusting the states of secondary switches. Combining the *LLC* converter with one of the rectifiers, a 250 W 38–120 V input, 500 V output prototype of one example is developed and tested, with a peak efficiency of 98.196%. Compared with similar *LLC* converters with secondary rectifiers, the proposed one's own a much wider gain range with fewer devices.

REFERENCES

[1] J. U. Duncombe, R. Beiranvand, B. Rashidian, M. R. Zolghadri, and S. M. H. Alavi, "Using LLC resonant converter for designing wide-range voltage source," *IEEE Trans. Ind. Electron.*, vol. 58, no. 5, pp. 1746–1756, May 2010.

[2] Q. Wu, M. Jiang, Z. Sun, and Q. Wang, "An internal magnetic core termination integration method for LLC four-elemental matrix transformer," *IEEE Trans. Power Electron.*, vol. 38, no. 11, pp. 13573–13579, Nov. 2023, doi: 10.1109/TPEL.2023.3304141.

[3] X. Sun, X. Li, Y. Shen, B. Wang, and X. Guo, "Dual-bridge LLC resonant converter with fixed-frequency PWM control for wide input applications," *IEEE Trans. Power Electron.*, vol. 32, no. 1, pp. 69–80, Jan. 2017.

[4] J.-B. Lee, J.-K. Kim, J.-I. Baek, J.-H. Kim, and G.-W. Moon, "Resonant capacitor on/off control of half-bridge LLC converter for high-efficiency server power supply," *IEEE Trans. Ind. Electron.*, vol. 63, no. 9, pp. 5410–5415, Sep. 2016.

[5] F. Alaql, A. Alhatlani, and I. Batarseh, "Multi-mode rectifier-based LLC resonant converter for wide input voltage range applications," in *Proc. IEEE Appl. Power Electron. Conf. Expo.*, 2021, pp. 349–354.

[6] H. Wu, Y. Li, and Y. Xing, "LLC resonant converter with semiactive variable-structure rectifier (SA-VSR) for wide output voltage range application," *IEEE Trans. Power Electron.*, vol. 31, no. 5, pp. 3389–3394, May 2016.

[7] F. Alaql, R. Rezaii, S. Gullu, M. T. Elrais, and I. Batarseh, "A switchable rectifier-based LLC resonant converter for photovoltaic applications," in *Proc. IEEE Energy Convers. Congr. Expo.*, 2021, pp. 2093–2098.

[8] M. Shang, H. Wang, and Q. Cao, "Reconfigurable LLC topology with squeezed frequency span for high-voltage bus-based photovoltaic systems," *IEEE Trans. Power Electron.*, vol. 33, no. 5, pp. 3688–3692, May 2018.

[9] H. Wang and Z. Li, "A PWM LLC type resonant converter adapted to wide output range in PEV charging applications," *IEEE Trans. Power Electron.*, vol. 33, no. 5, pp. 3791–3801, May 2018.

[10] Z. Sun et al., "A unified common inductor and common capacitor current sharing method for multiphase LLC converter," *IEEE Trans. Power Electron.*, vol. 37, no. 10, pp. 12182–12196, Oct. 2022.

[11] U. Ahmad et al., "Small-signal model and controller design of interleaved isolated boost converter for PV application," in *Proc. 48th Annu. Conf. IEEE Ind. Electron. Soc.*, 2022, pp. 1–6.

[12] E. H. Kim and B. H. Kwon, "High step-up resonant push-pull converter with high efficiency," *IET Power Electron.*, vol. 2, no. 5, pp. 79–89, 2009.

[13] J. M. Kwon, E. H. Kim, B. H. Kwon, and K. H. Nam, "High-efficiency fuel cell power conditioning system with input current ripple reduction," *IEEE Trans. Ind. Electron.*, vol. 56, no. 3, pp. 826–834, Mar. 2009.